Core Structure and its Association with Transformer Susceptibility towards Ferroresonance

C. A. Charalambous, Z. D. Wang, P. Jarman and M. Osborne

Abstract---**This paper particularly examines the transient electromagnetic performance of the core for a three phase 400/275 kV five limb and a three phase 400/275 kV three limb autotransformer, under normal and saturating conditions, by utilizing Finite Element techniques. This case study provides an insight on the level of saturation, under ferroresonance, that can be experienced by the various types of transformers of the UK's National Grid system, highlighting those units which are considered most vulnerable.**

Keywords: **Power Transformers, Saturation, Ferroresonance, Finite Element Modeling.**

I. INTRODUCTION

Ferroresonance is attributed to the interaction between the nonlinear characteristics of the transformer core with system's capacitance [1]. It is a low frequency phenomenon that may occur in a power transformer when one side of a double circuit transmission line connected to the transformer is switched out. The transfer of power from the adjacent energized line through capacitive coupling into the de-energized line could excite the unloaded transformer therefore saturating the core.

Core saturation will mean that the core flux density waveform will be non-sinusoidal and have a harmonic content giving rise to additional core loss, increased temperature rise and accompanying increase in noise level with unusual overtones present.

Moreover, in older transformer designs, the main limbs, yokes and any 4th and 5th limbs are held together with core tie bolts which pass through the whole core stack. These core bolts can pose a particular danger during core saturation events.

The autotransformer units of National Grid UK can have either a three-limb or five-limb core. The three limb core has one phase on each core limb, while the five limb core structure has three main limbs carrying the windings. The outer 4th and 5th side limbs act as return paths connecting the top and bottom yokes.

This case study particularly examines the transient electromagnetic performance of a three phase 400/275 kV five limb and a three phase 400/275 kV three limb autotransformer under normal and saturating conditions, using the Finite Element software – slim [2]. The main objective is to identify the susceptibility of the core of these two different structures towards ferroresonance.

II. TRANSFORMER CHARACTERISTICS

The autotransformers' basic information is tabulated in Table I. The core of both transformers is made out of Unisil steel 27M4. Fig. 1 illustrates the material's characteristic curve, as obtained from the manufacturer, on a semi-log plot. The physical dimensions of the structures, i.e. core limb and yoke, winding, insulation clearance and other structural parts were available from manufactures' design data sheets. The test reports of these transformers were also available.

TABLE I
AUTOTRANSFORMERS' CHARACTERISTICS

Units Description	SGT1	SGT2
Rate - HV/LV	1000 MVA - 400/275 kV	1000 MVA - 400/275 kV
Tertiary	Yes	Yes
Limbs - %Ratio	(5) - 60/60/100	(3) - 100/100
Type – Vector	Auto - Yy0	Auto - Yy0
Manufactured Year	1996	1980
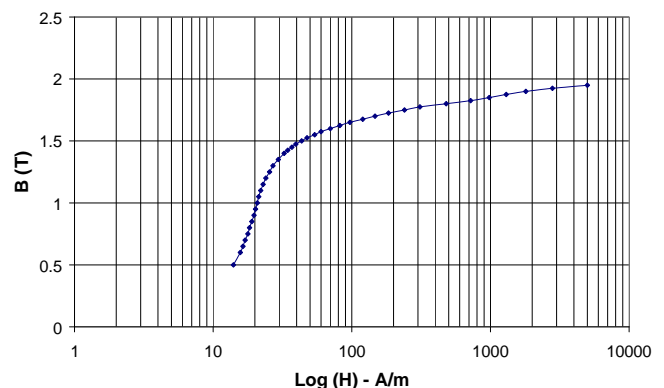
Fig. 1. Unisil 27M4 Steel Characteristics

C. A. Charalambous and Z. D. Wang are with School of Electrical and Electronic Engineering at The University of Manchester, PO BOX 88, Manchester M60 1QD UK. (charalambos.charalambous@manchester.ac.uk and zhongdong.wang@manchester.ac.uk).P. Jarman and M. Osborne are with National Grid, Warwick Technology Park, Gallows Hill, Warwick CV34 6DA UK.

III. SIMULATION MODEL DESCRIPTION

A. *Existing Relevant Simulation Practices*

An important aspect to accurately assess the core state under normal or most importantly saturating conditions is the topologically correct representation of the core. The researchers' efforts so far, have been focused in developing mathematically adequate transformer models for computer transient simulations, many of which require significant approximations to account for the absence of correct topology of the limbs [3]. A characteristic validated application of the latter type of models can be found in [4]. In [4] although attaching the non-linear effect externally to the model is an approximation, it is reasonably accurate for frequencies below 1 kHz.

Moreover, the detailed transformer models described in literature, which have reflected on the importance of accurate representation of the core, are primarily based on the principle of duality [5]. Utilizing this principle the developed transformer models can incorporate the saturation effects of the limbs and the yoke separately and further on they can account for the leakage effects and the capacitive coupling [6].

However, the complexity of a transformer's geometrical structure still poses a challenge for researchers to understand the flux redistribution during core saturation [7]. For the context of this paper it is imperative to use a model that is able to provide visual evidence of the core state both under normal and ferroresonance conditions. This has been achieved through the use of slim electromagnetic software [2].

A transient time domain analysis was carried out by using geometrically accurate two dimensional models; one for the three limb transformer and one for the five limb transformer, under the same exciting conditions. Specifically, the transverse view models, shown in Fig. 2 are used to establish the level of core saturation under the same ferroresonance conditions, as will be detailed.
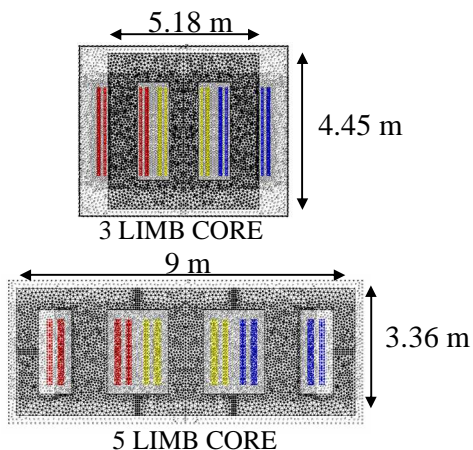

Fig. 2. Finite Element Mesh for 3 and 5 limb core transformers (2D transverse view)

B. *Ferroresonant Conditions Imposed*

In the finite element simulations, a small time step is necessary in order to model accurately the rapidly changing waveform, especially when dealing with peaky ferroresonant currents (fundamental mode). Unfortunately, any available field measurements of voltage and current were made only every 1 ms, too crude for use directly in the finite element calculation. Instead, it was necessary to make a cubic-spline fit (whose output was fine enough to be suitable for use in the finite element calculation) to the field test data waveforms and use the cubic-spline as the input to the time domain analysis.

Typical field ferroresonant current waveforms such as the ones modeled (curve fitted) were described in [4]. These correspond to the same type of transformers as those utilized in this case study. It should be clarified that the same ferroresonant current waveforms were imported to the finite element solver, for both three limb and five limb model structures.

C. *Finite Element Modeling Specifics*

The software used, calculates the winding flux linkage by utilizing the vector magnetic potential, expressed in Wb/m – flux divided by the length in the direction of the vector component considered and the current component producing it. The windings are treated as current sources and are assumed to be sufficiently finely stranded and transposed so that no eddy currents are induced in them. The relationship between winding flux linkage and average vector potential is given in [9].

Furthermore, within the 2D magnetic field solvers employed, stacking factors are utilized to modify permeability values in the 3 Cartesian directions. The user specifies values of relative permeability for linear materials or BH data files for non-linear materials, as in this case. Consequently, directional anisotropy in the core is modeled via stacking factors [10]. For the purpose of this study the stack factors utilized are: $sf_x = 1$, $sf_y = 1$ and $sf_z = 0.97$ for the x-y-z directions respectively. It should be noted however, that the directional permeabilities will not significantly influence the leakage flux and in the case they are ignored this will give a pessimistic result.

Lastly, for these finite element studies the tank was not modeled explicitly, but instead was represented by a constrained (flux line) boundary. This constraint boundary would not allow any flux to escape beyond the tank inner surface.

IV. SIMULATIONS

For Y connected 400 kV windings the line current is the same as the phase current; the current waveforms (normal and ferroresonant) were used to provide the excitation, i.e. the amp-turn product on the 400 kV winding, for the transient studies of the models in Fig. 2.

A. Steady State Conditions

Prior to ferroresonance currents injection, the 50Hz magnetising current, as found in the test reports, has been injected at the 400 kV side. This study serves the scope of calibrating the core to account for all the small gaps at the joints of the core laminations, which are unavoidable during core manufacture. More specifically, according to test reports the magnetising current of 0.363 A rms at the 400 kV side would produce a peak flux density of 1.7 T, for the 5 limb core. As far as the 3 limb core is concerned, the three phase 50Hz magnetising current of 0.167 A rms at the 400 kV side would produce a peak flux density of 1.7 T.

To align the model with the practical condition of the manufactured core, a modelling trick was applied. This has been achieved by stretching the B-H curve. This method can incorporate the effect of the air gaps (equivalent to step-lapped joint) inserted across the yokes and outer limbs. The principle is to scale the B-H curve until the calculated open circuit voltages, are matched with the design's sheet open circuit voltages. It should be noted that this is one way of calibrating the overall reluctance of the core model. However, the shortcoming of this method is that any local flux escape, at the joints, may not be accurately represented.

The magnetostatic studies performed have deduced a scale factor of 1.4 for the five limb core and 1.1 for the three limb core. This means that the magnetic field strength - H values of the B-H characteristics of Unisil 27M4 were scaled (stretched) by 1.4 and 1.1 times for the five and three limb cores respectively. Fig. 3 illustrates the resulted time modulus of the flux density distribution in both core models at zero phase angle under normal magnetising conditions; Phase R being the reference phase. It should be noted that the scale factor of the 3 limb core is, as expected, lower - reflecting the fewer joints present in the core.
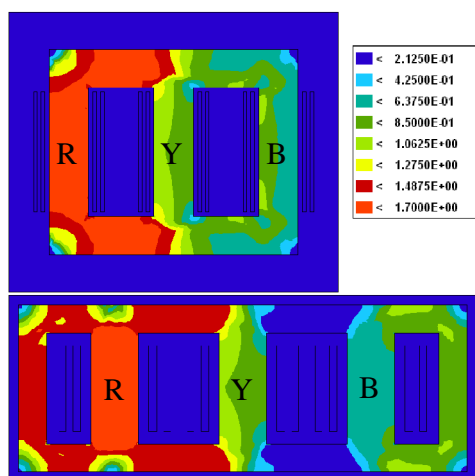

Fig. 3. Time Modulus of Flux Density Distribution within the Core

B. Ferroresonant Conditions

National Grid experience suggests that the sustained fundamental mode of ferroresonance is the most severe case due to the high energy transferred to the transformer.

Referring to [4] an approximate ratio of 1:2:1 for R:Y:B exists for the fundamental mode sustained ferroresonance voltages and currents of the three phases. Phases R and B are in anti-phase with phase Y, suggesting that all the three phase limbs would become highly saturated at the same instant. For the purpose of this paper, the sustained ferroresonant currents of the unloaded transformer have been used in the subsequent studies.

When the line currents of the transformer are added up, borrowing the steady-state convention, $3I_0 = I_R + I_Y + I_B$, the zero sequence current $3I_0$ in this particular scenario is negligible compared to the magnetization current. However, in cases where this sum is not negligible, the tertiary winding ought to be modeled to allow any zero sequence currents to circulate within it. It should be noted that provision of a tertiary winding on the 5-limb core would drastically alter the zero sequence impedance, since zero sequence currents would be able to circulate around the delta tertiary winding and thus balance those flowing into the primary winding.

The modeling of the tertiary winding becomes possible, within the software used, by using an external schematic capture tool to add the necessary windings into the circuit as a separate entity [8]. Therefore the currents can be induced in the tertiary by the calculated fields.

Moreover, the Finite Element Analysis solution, for this scenario, was carried out for 10 cycles (0 – 0.2 seconds). Specifically, the time domain magnetic 2D solver works by performing a transient solution at each point in time, utilising the excitation data corresponding to that specific time instant. The induced currents are calculated from the differences between the magnetic vector potentials of the present time step and the previous time step.

The transient solution provides graphical snapshots of the core flux density distribution at each time step. It should be noted at this point that the pattern presented by Fig.s 4 and 5 are periodic for the case of fundamental mode sustained ferroresonance. This means that the same pattern is repeated in a 50Hz cycle. Fig. 4 illustrates the flux density distribution for the three limb and five limb core structures.

The snapshot presented corresponds to the time step at which all 3 phase ferroresonant currents are at their minimum values. It can be observed that there is no evidence of core saturation in neither of the two structures. However, the flux density in the yokes of the five limb structure is considerably higher (20%) than in the yokes of the three limb structure.

Fig. 5 illustrates the flux density distribution which corresponds to the time step at which all 3 phase ferroresonant currents are at their maximum values. The plots reflect the worst saturating conditions deduced by the Finite Element Solution. The centre limb of the three limb structure is saturated near 2.15 T, while the saturation of the outer limbs is less, around 1.9T. As far as the five limb structure is concerned, all three main limbs are highly saturated, while

the outer limbs are also considerably saturated. One can also observe that the yokes of the five limb structure are significantly saturated as opposed to the yokes of the three limb structure, where there is no evidence of saturation.
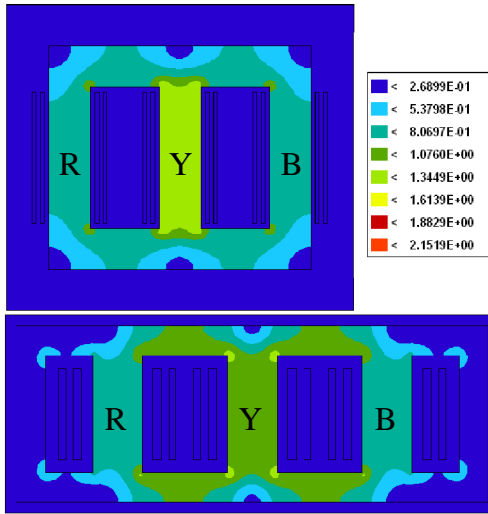

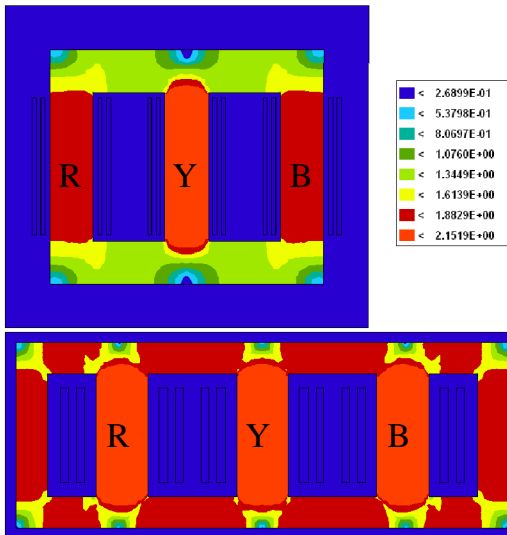Fig. 4. Flux Density Distribution – Ferroresonant Currents (R:Y:B -1:2:1)at their minimum values.

Fig. 5. Flux Density Distribution – Ferroresonant Currents (R:Y:B -1:2:1)at their maximum values.

It is perhaps more instructive to study the space average permeability value for each element of the core limbs at each instant time, as an index of the overall saturation of the limb/yoke area. Fig. 6 illustrates a comparison of the time space average permeability of the core limbs for the three limb and five limb structure respectively. The space average value of the permeability was found for each element averaged over the area occupied by the core limbs.

Fig. 6 reveals that the lower average space permeability, which encapsulates the core saturation state, can be the same for both structures. However, the five limb structure can maintain this low permeability value for longer time. It is evident on Fig. 6 that the average space permeability

distribution of the three limb structure is sharper (peaky) implying that the core limbs maintain that low permeability value for shorter time, i.e. the peak saturation time is shorter.

Fig. 7 illustrates a comparison of the time space average permeability of the yokes for the three limb and five limb structures respectively, as described previously.

The lower permeability value of the yoke of the five limb structure is considerably lower than that of the three limb transformer. Moreover the duration for lower permeability state, is increased which indicates that the yoke saturation in a five limb structure is deeper and furthermore is maintained for longer time.
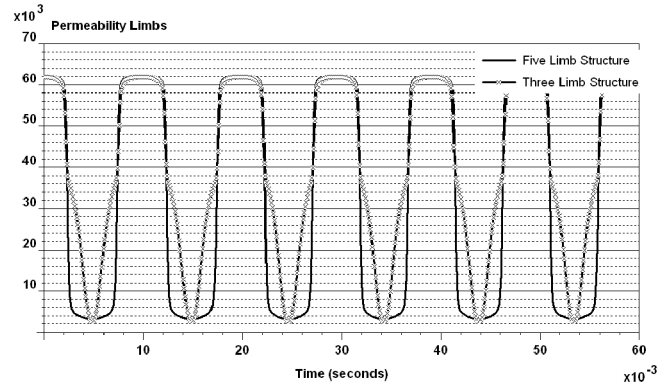

Fig. 6. Limbs Space Average Permeability Value over time (R:Y:B - 2:1:1)
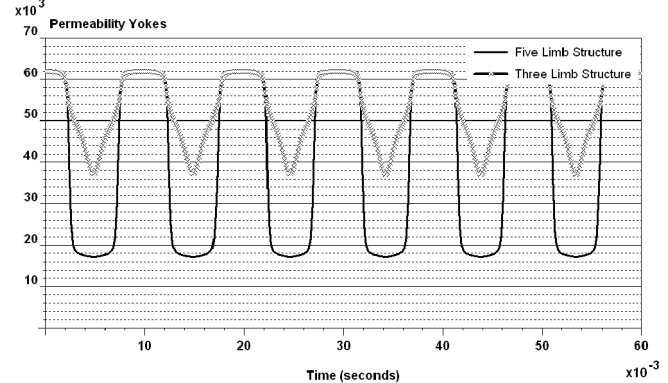

Fig. 7. Yoke Space Average Permeability Value over time (R:Y:B - 1:2:1)

C. Sensitivity Studies

In the event of fundamental mode ferroresonance occurrence, the literature reveals cases where phases Y and B are in anti-phase with phase R (an approximate ratio of 2:1:1 for R:Y:B) [7], in addition to the scenario presented in section B (1:2:1 for R:Y:B). Fig. 8 illustrates the flux density distribution which corresponds to the time step at which all 3 phase ferroresonant currents are at their maximum values, corresponding to the scenario (2:1:1 for R:Y:B). The plots reflect the worst saturating conditions deduced by the Finite Element Solution, as it was the case in section B.

By comparing Figs 5 and 8 it can be observed that there is a considerable difference in the pattern of the flux density distribution, even though the maximum flux density is maintained around 2.15 T. Specifically in the case of the

three limb structure, the maximum flux density appears to be on the limb labeled R. i.e. the limb that its windings carry the maximum current. Interestingly enough, in this case scenario a section of the yoke is considerably saturated (2.09 T) as opposed to the previous case study. Sections of the yoke are also highly saturated and in the case of the five limb structure, when compared with Fig. 5. Also, the highly saturated yoke forces the flux to escape, in the area between limbs Y and B, into the insulation space.

Fig. 9 illustrates a comparison of the time space average permeability of the core limbs for the five limb and three limb structures, respectively. By comparing Fig.s 6 and 9, it can be observed that the peak saturation time of the five limb structure for R: Y: B - 2:1:1 is now reduced as opposed to the ferroresonance current ratio R: Y: B – 1:2:1. This is evident from the average permeability distribution which is sharper (peaky) implying that the core limbs maintain that low permeability value for shorter time, i.e. the peak saturation time is shorter.
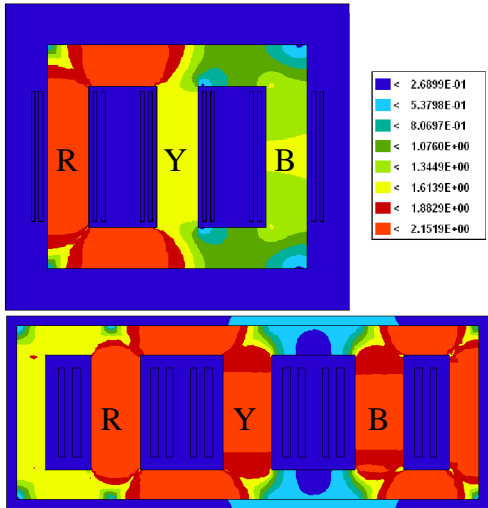

Fig. 8. Flux Density Distribution – Ferroresonant Currents (R:Y:B -2:1:1) at their maximum values.

As far as the three limb structure is concerned, a considerable increase is noted for the minimum limbs' permeability reached, in favour of the ferroresonance current R:Y:B – 2:1:1.
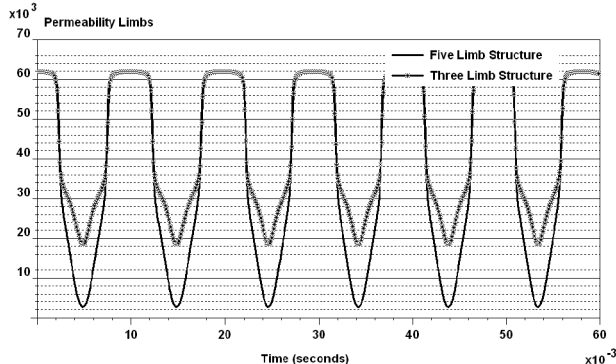

Fig. 9. Limbs Space Average Permeability Value over time (R:Y:B - 2:1:1)

Fig. 10 illustrates a comparison of the time space average

permeability of the yokes for the five limb and three limb structures, respectively. Specifically, in the three limb structure of the R: Y: B - 2:1:1 ferroresonance scenario, is there exists a decrease in the minimum permeability value reached. In this particular case, it is evident that the time duration that the yokes can maintain the lowest permeability value is now increased for both structures as opposed to Fig. 7.

Lastly, table II summarizes the minimum average space permeability ratio when assessing the two ferroresonance scenarios, i.e. R:Y:B - 1:2:1 and R:Y:B - 2:1:1. It should be noted that when the calculated ratio is less than 1, the limbs (or the yokes) are more saturated (i.e. lower permeability) in the ferroresonance scenario R:Y:B - 1:2:1. On the contrast, if the ratio is greater than 1 the limbs (or the yokes) are more saturated in the ferroresonance scenario R:Y:B - 2:1:1.
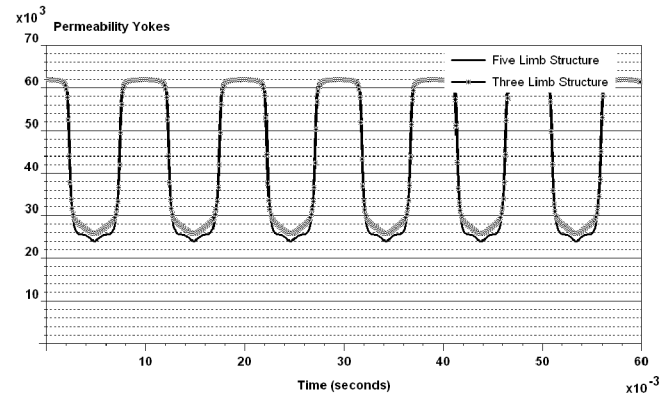

Fig. 10. Yokes Space Average Permeability Value over time (R:Y:B - 2:1:1)

TABLE II
MINIMUM AVERAGE SPACE PERMEABILITY RATIO

	FIVE LIMB STRUCTURE Minimum Permeability Ratio R:Y: B – (1:2:1 / 2:1:1)	THREE LIMB STRUCTURE Minimum Permeability Ratio R:Y: B – (1:2:1 / 2:1:1)
LIMBS	$\dfrac{3.85\times10^3}{2.5\times10^3}$	$\dfrac{3.82\times10^3}{18\times10^3}$
YOKES	$\dfrac{16.9\times10^3}{24\times10^3}$	$\dfrac{36.7\times10^3}{26\times10^3}$

D. Discussion Of Results

The different core types are examined in this paper i.e. the three limb and the five limb transformer. The difference on their flux distribution behavior under normal operating conditions has been a subject of research. Specifically in [11] it is stated that the flux distribution for the 3 limb cores is quite uniform since it is induced equally in the limbs and the flux from one phase is not competing with the flux of the other phases. As far as the five limb core is concerned the flux distribution is quite non-uniform even at normal operating conditions. When the flux is induced in one of the main limbs, it splits between the other two core limbs. This is evident on Fig. 3 of this paper.

Making a step further, this paper attempts to investigate the flux density distribution under saturating conditions

caused by ferroresonant currents, specifically when dealing with fundamental mode sustained ferroresonance.

Although, both three limb and five limb models have been excited from the same set of ferroresonant currents, the degree and distribution of saturation varies appreciably. The difference on the degree of saturation, (encapsulated in the average space permeability pattern and in flux density distribution), is attributed partly to the relatively small yoke dimension of the five limb structure. These worst saturation conditions of the latter, not only include deeper but also longer periods of saturation, therefore constituting the five limb structure more susceptible to fundamental mode sustained ferroresonance.

It should be kept in mind however, that the flux density distribution within the core is also depended on how the ratio of the sustained mode ferroresonance current is allocated between the three phases. (1:2:1 or 2:1:1).

Lastly, it is highlighted that the results obtained, for this case study, are very depended on the accuracy of the B-H curve employed at high flux densities. There are rarely if ever any measurements at these highly saturated regions, therefore this paper has incorporated extrapolations from lower measured fluxing aiming for an ultimate slope of the permeability of free space.

V. CONCLUSIONS

This paper presented a case study carried out to understand and to provide evidence of the susceptibility, of the main types of transformers of National Grid, towards ferroresonance. It was deduced that the five limb core transformer is most susceptible to ferroresonance. Furthermore, it was specifically shown that limbs of the transformer are most easily saturated parts of the transformer core.

The conclusions are particularly useful as ferroresonance is believed to be a contributing factor to the eventual failure modes by exposing the transformer's components to electromagnetic and thermal stresses. Solid ferrous components such as core and yoke bolts will suffer eddy current losses made worst by the extreme saturating conditions, which if concentrated can give rise to high localized temperatures.

VI. ACKNOWLEDGMENT

VII. REFERENCES

[1] Slow Transients Task Force of the IEEE Working Group on Modeling and Analysis of Systems Transients Using Digital Programs, "Modeling and analysis guidelines for slow transients—part III: The study of ferroresonance," *IEEE Trans. Power Del.*, vol. 15, no. 1, pp. 255–265, Jan. 2000.

[2] SLIM version 3.9.1 ©, AREVA T&D October 2006, support.slim@areva-td.com

[3] Alternative Transients Program Rule Book. Heverlee, Belgium, K.U. Leuven EMTP Center, 1987.

[4] C. Charalambous, Z. Wang, M. Osborne, P. Jarman ''Validation of a Power Transformer Model for ferroresonance with system tests on a 400kV circuit'' I.P.ST 2007, Lyon, France 4th-7th June 2007.

[5] B. A Mork, ''Five-Legged wound core transformer model: Derivation, parameters, implementation and evaluation, '' IEEE Trans. Power Del.., vol. 14, no.4 pp. 1519-1526, Oct. 1999.

[6] B. A Mork, F. Gonzalez, D. Ishcenko, D. L. Stuehm, J. Mitra. '' Hybrid Transformer Model for Transient Simulation-Part I: Development and Parameters'', IEEE Trans. Power Delivery, Vol. 22, PP. 248-255, 2007.

[7] C. A. Charalambous, Z.D. Wang, P. Jarman, M. Osborne, '' Two-Dimensional Finite Element Analysis of an Auto-Transformer Experiencing Ferroresonance'', Accepted (Dec. 2008) to IEEE Trans. Power Del.

[8] Circuit Definition Technical Guidance SLIM version 3.9.1 ©, AREVA T&D October 2007, support.slim@areva-td.com

[9] Alessandra Sitzia, The relationship between winding flux linkage and average vector potential (Amean), Technical Note – Slim Technical Manual, 22 July 2003, AREVA T&D Technology Centre, Stafford, U.K.

[10] Alessandra Sitzia, Stacking Factors and Directional Permeabilities in SLIM Magnetic Solvers, Technical Note – Slim Technical Manual, 13 September 2005, AREVA T&D Technology Centre, Stafford, U.K.

[11] Ed G. teNyenhuis, Gunter F. Mechler, Ramsis S. Girgis, '' Flux Distribution and Core Loss Calculation for Single Phase and Five Limb Three Phase Transformer Core Designs'', IEEE trans. Power Del., Vol. 15, no. 1, January 2000.

VIII. BIOGRAPHIES

Charalambos A. Charalambous was born in Nicosia, Cyprus in 1979. He received a Class I BEng (Hons) degree in Electrical & Electronic Engineering in 2002 and a PhD in Electrical Power Engineering in 2006 from UMIST, UK (The University of Manchester). He is currently a Research Associate within the National Grid High Voltage Research Center in the University of Manchester, UK. His research interests include transformer finite element modeling, Ferroresonance transient studies, and the electrical control and analysis of DC corrosion.

Zhongdong Wang received a BEng and a MEng degree in High Voltage Engineering from Tsinghua University of Beijing in 1991 and 1993, and a PhD in Electrical Engineering from UMIST of UK in 1999. Since 2000 she is a Lecturer then a Senior Lecturer in the School of Electrical and Electronic Engineering at the University of Manchester. Her research interests include transformer modeling, transformer insulation materials and transformer asset management.

Paul Jarman was born in London in 1962 and graduated from Cambridge University in 1984 with an Honours Degree in Electrical Science. He joined the Central Electricity Generating Board, Research Division where he worked on projects including loss measurement instrumentation for bushings and FRA techniques for transformers. In 1990 he joined the National Grid Substations Section as a Transformer Engineer becoming Head of Transformers in 1998. Since 2001 Paul has been the Technical Specialist for transformers within National Grid Transco's Asset Strategy group. The group has responsibility for technical policy, asset stewardship and engineering support. He is a chartered electrical engineer and member of the IET.

Mark Osborne was born in South Africa in 1969. He graduated from Lancaster University with a Physics honours degree and completed his doctorate at the University of Sunderland in 1997 in 'Computer based analysis of Custom Power Technology'. He works in the Asset Management section of National Grid UK Transmission. His areas of interest include insulation coordination, substation design and policy development.